

MOLECULE CONFIGURATIONS IN A DROPLET DETACHMENT PROCESS OF A SEMDILUTE XANTHAN SOLUTIONS

Christian Wagner* and Andriy Kityk**

*Experimentalphysik, Universität des Saarlandes, Postfach 151150, 66041 Saarbrücken, Germany

**Institute for Computer Science, Technical University of Czestochowa, Armii Krajowej 17, 42-200 Czestochowa POLAND

Summary The detachment process of a droplet of an elastic liquid is characterized by the suppression of the pinch off finite time singularity and the formation of a cylindrical filament between the droplet and the nozzle. The flow in this filament is purely elongational. The resistance to such a flow is macroscopically described by the elongational viscosity. However, a sound understanding of the functional connection between the microscopic configurations of the macromolecules and the macroscopic flow is still missing. We present birefringence data that are taken simultaneously to the macroscopic flow measurements. By changing the ionic strength of the solvent we can tune the flexibility of our polyelectrolytic macromolecules and correlate them with the microscopic polymer configurations and the measurements of the elongational viscosity.

SUMMARY

The detachment process of a droplet of a simple liquid is characterized by a finite time singularity of the minimum neck diameter¹. However, the addition of a tiny amount of flexible polymers can lead to the suppression of the finite time singularity². At a given moment t_c the flow - or strictly speaking its elongational parts - becomes strong enough to deform the polymers and a sharp transition from the self similar power law to a much slower exponential dynamic takes place. A cylindrical filament connecting the droplet and the reservoir is formed and the according flow profile is purely elongational. The resistance to such a flow is macroscopically quantified by the elongational viscosity η_e . It is known that flexible polymers have a higher elongational viscosity than stiff molecules, but the underlying physical mechanisms are only poorly understood. It is thus reasonable to study both the microscopic confirmation and the macroscopic flow response as a function of the chain flexibility. This is possible by using polyelectrolytic polymers, for which the chain flexibility can be tuned by the addition of salt to the solvent³. In that way the chain flexibility is altered *without* changing either the polymer chemistry or the chain length (the effects of which on the elongational viscosity are still ill understood).

The polymer we use is Xanthan (Sigma-Aldrich, Mw:~3Mio) at a weight concentration of 500ppm dissolved in 80wt% glycerol-water. The ionic strength of the solvent is tuned by the addition of KCl at concentrations ranging from 0 to 0.1wt%. Xanthan has a high optical anisotropy and due to its shear thinning effects (and its biological digestibility) it is used largely in the food, pharmaceutical, oil and cosmetic industry.

The experimental setup is sketched in figure 1. The sample solution is quasistatically driven by a syringe pump through a nozzle with a diameter of $d=2\text{mm}$. In a distance $D=7\text{cm}$ below the nozzle a plate is mounted in order to omit gravitational effects in the thinning process of the filament. The Retardation δ is measured by use of the optical train consisting of a 5mW HeNe Laser, a Polarizer P, a photo acoustic modulator PAM, the sample liquid, an Analyzer A, a bright field lens system and a photo diode connected to two Lock-Ins. The polarizer is fixed at an angle of 45° relative to the photoelastic modulator. The photo acoustic modulator allows for a Lock-In technique for the detection of the retardation signal. The bright field lens system (figure 1 B) in front of the detector prevents any light that has not passed the filament from reaching the detector by blocking the parallel components with a mask M in the focal point of lens L1⁴. The lens L2 collects the light that is diffused by the cylindrical filament into the detector.

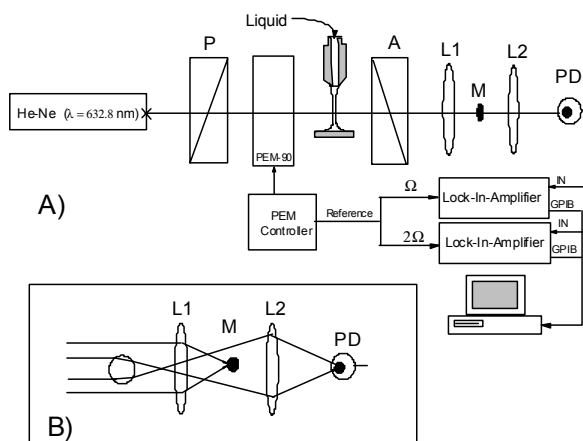


Figure 1

The experimental setup. See text for explanation.

To calculate the birefringence from the retardation signal the instantaneous thickness $h(t)$ of the filament must be known. Therefore the thinning process of the minimum filament diameter h is measured with a high speed camera (encore mac PCI 1000S) that is placed perpendicular to the optical train. The camera is equipped with a 2 times magnification objective and the image capturing is synchronized to the data collection of the two Lock-In's. The data of $h(t)$ for different salinities are shown in figure 2 a). A decrease in salinity leads to a faster dynamic, hence to a lower resistance of the polymers to the flow. The data can be directly used to calculate the elongational viscosity η_e by equating the capillary pressure with the elastic stresses. Recently Anna and Mc Kinley have shown that "filament thinning studies and filament stretching form complementary experiments" that lead to consistent measures of the transient extensional viscosity of the fluid⁵. The elongational viscosity η_e is time dependent because in the course of the experiment the polymers are more and more stretched by the flow. The experiments reveal that the temporal behavior of $h(t)$ is first exponential, implying that the elongational rate $\dot{\epsilon} = -2\partial_t h/h$ remains constant. This indicates a subtle interplay between the polymer and the flow dynamic. For large times of course a steady state value of the elongational viscosity $\eta_e = \text{const}$ will be reached that depends only on the elongation rate $\dot{\epsilon}$. Figure 2 b) shows that the elongational viscosity decreases with increasing salinity. This correlates with a decrease in flexibility of the polymer chains. Different than most polyelectrolytes Xanthan stiffens with increasing ionic strength due to a collapse of the sugar-backbone.

The microscopic confirmation of the macromolecules can be studied by use of the birefringence data. The birefringence signal is proportional to the end to end elongation of the molecules, to their orientation and to the concentration. In elongational flow the polymer should be elongated along the flow and thus the birefringence is proportional to the elongation of the polymers and the concentration. In that way we could test our method by performing several runs at different polymer concentrations and the birefringence signal was always proportional to the concentration.

The data in figure 3 c) were taken for different salinities and one observes that the birefringence at higher salinities and thus for stiffer polymers is larger than for more flexible ones. This confirms the physical picture that stiffer polymers are already at equilibrium more elongated. However, they perform a lower resistance against the flow as we have shown in figure 2 b). The functional behavior of the birefringence signal shows a monotonic increase that correlates with the uncoiling of the polymer. However at the final stage of the experiment, we observe a divergence in the birefringence signal. This divergence is very robust and takes place at stages of the filament thinning process when the filament diameter is still large enough to render the analysis unambiguous. While the polymers should be completely uncoiled at this stage of constant steady state elongational viscosity we can attribute this behavior only to a concentration enhancement. This explanation is supported also by the fact that eventually the filament might not break at the final stages of the thinning process but a very thin polymer fiber remains between the nozzle and the ground plate.

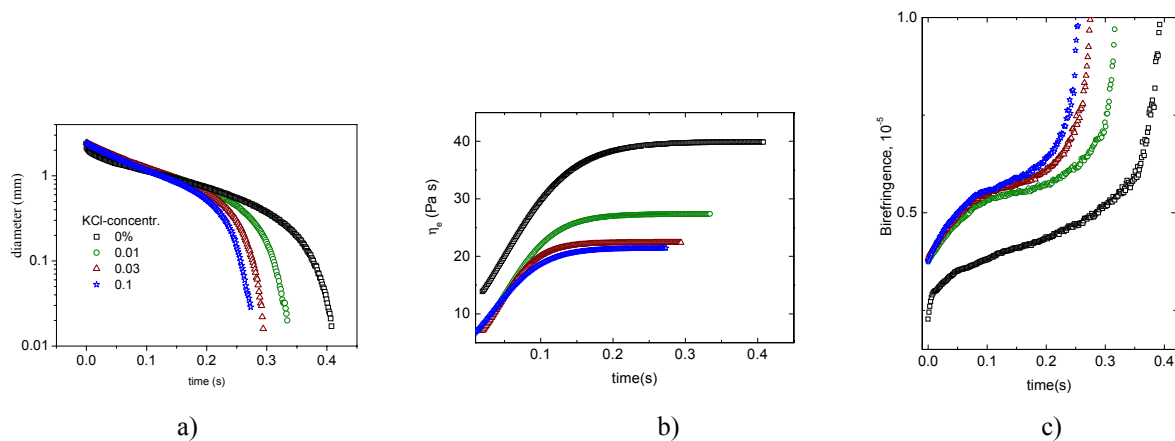


Figure 2

a) The filament diameter versus time. b) The time dependent elongational viscosity. C) The birefringence. All plots show data from runs at different ionic strengths of the solvent.

¹ For a review see: J. Eggers, Rev. Mod. Phys. 69, 865 (1997)

² Y. Amarouchene, D. Bonn, J. Meunier, and H. Kellay, Phys. Rev. Lett. **86**, 3558 (2001)

³ C.G. Bauman, S.B. Smith, V.A. Bloomfield, C. Bustamante, P.N.A.S. **94**, 6185 (1997)

⁴ T.Sridhar, D.A.Nguyen and G.G. Fuller, J. Non-Newt. Fluid-Mech. **90**, 299 (2000)

⁵ S. L. Anna, G. H. McKinley, J. Rheol. **45**, 115 (2001)